Insights into the binding of agonist and antagonist to TAS2R16 receptor: a molecular simulation study

Zhirong Chen, Shifen Dong, Fancui Meng, Yaoyue Liang, Shuofeng Zhang & Jianning Sun

View supplementary material

Published online: 28 Sep 2017.

Submit your article to this journal

Article views: 981

View related articles

View Crossmark data

Citing articles: 8 View citing articles

Taylor & Francis
Taylor & Francis Group

🔓 OPEN ACCESS | Check for updates

Insights into the binding of agonist and antagonist to TAS2R16 receptor: a molecular simulation study

Zhirong Chen[a], Shifen Dong[a], Fancui Meng[b], Yaoyue Liang[a], Shuofeng Zhang[a] and Jianning Sun[a]

[a]Department of Pharmacology of Chinese Medicine, Beijing University of Chinese Medicine, Beijing, China; [b]Tianjin Key Laboratory of Molecular Design and Drug Discovery, Tianjin Institute of Pharmaceutical Research, Tianjin, China

ABSTRACT

The human bitter taste receptors (TAS2Rs) belong to the GPCR family, while the activation mechanism and how TAS2Rs recognise bitter ligands are poorly understood. In this study, 3D structure of TAS2R16 was constructed using homology modelling complemented with molecular dynamics method. Salicin and probenecid were docked to TAS2R16 receptor to investigate the possible activation mechanism of TAS2R16. The results show that salicin and probenecid locate at the binding pocket made up of transmembrane helices TM3, TM5 and TM7, and the second and third extracellular loops ECL2 and ECL3. Structural analysis reveals that the network interactions at the third intracellular loop ICL3 may play a crucial role in stabilising the inactive state of TAS2R16, and structural change in the intracellular region is correlated with the activation of TAS2R16. The binding energies of salicin and probenecid to TAS2R16 are −152.81 ± 15.09 and −271.90 ± 26.97 kJ/mol, respectively, indicating that a potential antagonist should have obviously stronger binding affinity.

1. Introduction

Bitter taste signalling in humans is mediated by a group of bitter receptors (TAS2Rs) that belong to the G-protein coupled receptor (GPCR) family. It has long been assumed that bitter taste evolved as a defence mechanism to detect potentially harmful toxins in food [1]. Although a moderate bitter taste of food items known to be safe for consumption is frequently enjoyed, the recognition of potentially harmful food components is believed to be important for survival and well-being of vertebrates [2]. TAS2Rs are able to perceive a plethora of bitter substances with versatile structures [3]. The most divergent regions between TAS2Rs are the extracellular segments [4], which are thought to be responsible for recognition of structurally diverse ligands.

TAS2R16 is present in taste receptor cells on the tongue and can be activated by bitter compounds consisting of a hydrophobic residue attached to glucose by a β-glycosidic bond [5]. As many other bitter taste receptors, the experimental 3D structural information of TAS2R16 is also unavailable up to now. Homology modelling, complemented with molecular docking, provides a practical tool for building of the 3D structure of receptor and elucidating the binding mode of receptor and its ligands. In recent years, such approaches have been used to elucidate the structures of several members of the TAS2Rs, including TAS2R1 [6], TAS2R4 [7,8], TAS2R10 [9], TAS2R14 [10] and TAS2R38 [11]. With the development of computational tools, molecular dynamics (MD) simulation has also been used to understand the conformation changes of TAS2Rs upon ligand binding. Dai

et al. [6] performed MD simulations on TAS2R1 and found that the intracellular loop II (ICL2) and transmembrane helix TM3 might play prominent roles in the activation process of TAS2R1.

Better understanding of TAS2Rs-ligand recognition may be helpful for rational design of functional foods. To this end, in this study, the structure of TAS2R16 was constructed and the activation mechanism was investigated using MD simulations. Salicin was selected as an agonist since TAS2R16 could specifically respond to it. Probenecid, which has been proved to inhibit TAS2R16 and suppresses bitter perception of salicin [12], was selected as an antagonist for calculation.

2. Computational details

2.1. 3D structure building of TAS2R16

As the structure of TAS2R16 is unresolved, homology modelling method was used to construct its structure. The amino acid sequence of hTAS2R16, coded as Q9NYV7, was downloaded from UniProt database (https://www.uniprot.org). The crystal structure of β2 adrenergic receptor-Gs protein complex with PDB code 3SN6 [13] was selected as template protein (supporting information SI and SII). Sequence alignment and 3D structure building of TAS2R16 were carried out using Prime module of Schrödinger software [14]. Energy minimisation was performed on the obtained structure. Then, the structure of TAS2R16 receptor was embedded in a pre-equilibrated DPPC (dipalmitoyl phosphatidylcholine) system made up of 256 DPPC

lipids and 12,800 water molecules using g_membed tool [15], and the orientation of 3SN6 in membrane [16] was taken as the reference position. Counter ions were added to neutralise the whole system. The final system includes TAS2R16 protein, 244 DPPC lipids, 12,734 water molecules and 11 chlorine ions.

Molecular dynamics simulations were carried out in GROMACS 5.1 software [17,18] with AMBER03 force field. The force field parameters used for DPPC were derived by Jämbeck and Lyubartsev [19], which could be used together with the AMBER force field of proteins. TIP3P water molecules were used. Energy minimisation was performed on the system, followed by a 100 ps NVT and a 100 ps NPT MD (molecular dynamics) simulations with position restrictions on protein. MD production simulation was carried out for 50 ns with a time step of 2 fs. The trajectory was saved every 40 ps. The temperature was kept at 323 K using V-rescale method, and the pressure was controlled semi-isotropically using Parrinello-Rahman coupling method. The cut-off distances for electrostatic and van der Waals interactions were set to be 1.2 nm. Long-range electrostatic interaction was considered using particle mesh Ewald method. The obtained trajectory was analysed to assure that the system was well equilibrated. The equilibrated structure of TAS2R16 was taken out for further docking calculations.

2.2. Molecular docking of salicin and probenecid

The obtained conformation of TAS2R16 was adopted as the receptor to produce the Glide grid file for docking. SiteMap module was used to identify the top-ranked potential receptor binding site. The receptor grid was generated using the obtained binding site with a box size of 20 Å. The structures of two ligands (salicin and probenecid), whose structures were shown in Figure 1, were prepared using LigPrep with OPLS-2005 force field. Molecular docking calculations were carried out using induced fit docking [20] with default parameters. All these calculations were carried out in Schrödinger software.

2.3. Molecular dynamics simulations of salicin and probenecid

Two TAS2R16 complexes obtained by induced fit docking were embedded in the pre-equilibrated DPPC system. RESP (restrained electrostatic potential) method was used to produce the topology parameters of salicin and probenecid at B3LYP/6-31G(d,p) level. The MD simulations also lasted for 50 ns. The simulation steps and parameter set-up are the same as for TAS2R16 of *2.1*.
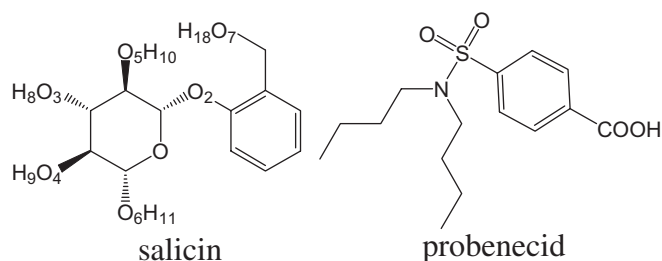

Figure 1. Chemical structures of salicin and probenecid.

All analyses were performed using the last 10 ns trajectories, otherwise specified. g_hbond tool of GROMACS was used to perform hydrogen bond analysis with default criteria, i.e. the donor-acceptor distance is less than 0.35 nm and the hydrogen-donor-acceptor angle less than 30°. The binding free energies between TAS2R16 and different ligands were calculated using MM-PBSA (Molecular Mechanics–Poisson Boltzmann Surface Area) method. g_mmpbsa [21], which implements the MM-PBSA approach using subroutines sourced from the GROMACS and APBS packages, was used. The selected non-polar solvation model is based on the solvent accessible surface area (SASA) with surface tension parameter $\gamma = 0.0226778$ kJ/mol.$Å^2$, $\beta = 3.84982$ kJ/mol, and probe radius 1.4 Å.

3. Results and discussion

3.1. Homology modelling of TAS2R16

Figure 2 shows the sequence alignment of TAS2R16 with PDB 3SN6. Ramachandran plot was often used to test the reasonability of homology model, providing an easy way to view the backbone dihedral angles Ψ against Φ of amino acid residues in protein structure. One can determine which torsional angles are permitted through a Ramachandran plot. The Ramachandran plot of TAS2R16 is shown in Figure S2, from which one can see that most of the residues occurred in the favoured or allowed region, and only 3 of 291 residues appeared in disallowed region. Therefore, our built 3D structure of TAS2R16 consisting of residue 1 to 291 is reasonable. In order to test its reliability and stability, molecular dynamics simulation has been performed on it.

3.2. Molecular dynamics of TAS2R16

The stability of TAS2R16 homology model was analysed by calculating the RMSD (root mean square deviation), radius of gyration (Rg) and RMSF (root mean square fluctuation). The RMSD analysis of the backbone atoms showed a rapidly increase to 0.3 nm in the first 10 ns, then fluctuated around 0.34 nm, and finally achieved a steady plateau after 30 ns (Figure 3(A)), indicating the TAS2R16 model attained equilibration during MD simulation. The Rg value of TAS2R16 was found to decrease to 2.13 nm at 15 ns, and then reached to a relatively steady value (Figure 3(B)), suggesting good compactness. RMSF analysis showed that most of the residues had a value less than 0.3 nm and the most flexible regions corresponded to the loop regions. The C-terminal region displayed the largest RMSF value (Figure 3(C)).

3.3. Molecular docking of ligands

The TAS2R16 protein was taken out from the MD simulation result as the receptor for following molecular docking. Salicin and probenecid were docked into the active pocket of TAS2R16 receptor using induced fit docking method. The docking results are listed in Table 1, and the predicted binding modes of the two ligands are shown in Figure 4. Salicin acquires better glide score value than probenecid. van der Waals interactions dominate the whole interaction energies for these two systems. The coulombic energy plays a minor role for probenecid system, whereas it is equally important for salicin system because salicin creates

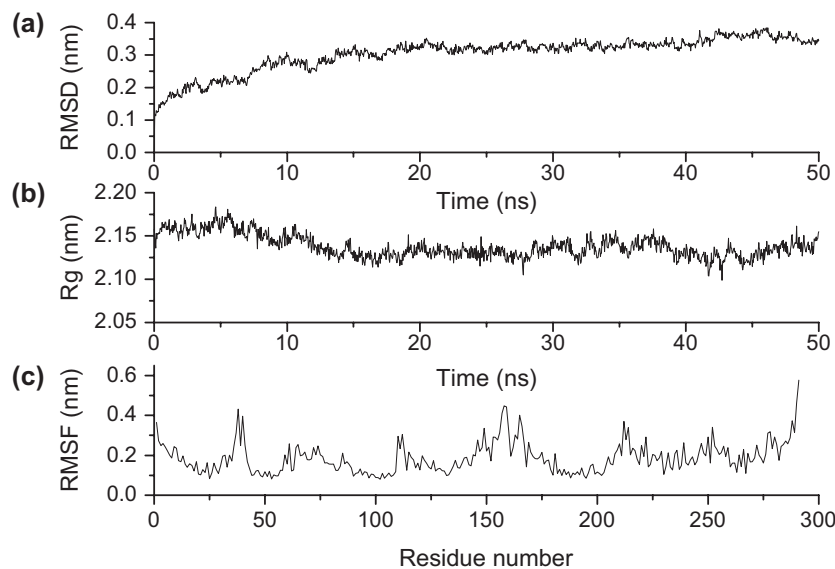**Figure 2.** (Colour online) Sequence alignment of TAS2R16 with PDB 3SN6.

Figure 3. Stability parameters of TAS2R16 homology model through 50 ns MD simulation. (A) RMSD of backbone atoms, (B) radius of gyration and (C) RMSF of each amino acid residues.

Table 1. Induced fit docking results.

Title	Docking score	Glide evdw	Glide ecoul	Glide energy	Prime energy	IFD-Score
Probenecid	−4.84	−25.33	−7.79	−33.11	−8667.5	−438.22
Salicin	−6.26	−24.87	−17.91	−42.78	−8387.4	−425.63

more hydrogen bonds than probenecid. However, probenecid obtains better estimated binding energy (IFDScore), suggesting that probenecid binds more tightly with TAS2R16 than salicin.

Salicin forms four hydrogen bonds with TAS2R16: one is between the carboxyl group of Glu86 and O6H11, with a bond length of 2.036 Å; another is between the carbonyl group of Asn89 and O4H9 with a hydrogen bond distance of 1.854 Å; the carboxyl group of Glu262 forms two hydrogen bonds with O7H18 and O5H10 with bond distances of 1.689 and 1.630 Å, respectively. The phenyl ring of salicin is stacked with His181 via $\pi-\pi$ interaction. There are several hydrophobic residues such as Ala184, Leu185, Leu244, Phe240 and Leu258 around the phenyl ring of salicin. As for probenecid, only two hydrogen bonds were formed: one is between the oxygen atom of sulfonic group and the amino group of Asn89, the other is between the carboxyl oxygen atom and Arg255. These two hydrogen bond lengths are 1.943 and 1.734 Å, respectively. The propyl groups of probenecid locate at the hydrophobic pocket formed by Phe93, Ala184, Leu185, Leu244 and Phe240, providing a better fit for the binding site on TAS2R16. Examining the binding modes of these two ligands with TAS2R16 receptor, it can be found that the binding pocket of TAS2R16 is made up of transmembrane helices TM3, TM5 and TM7, and the second and third extracellular loops ECL2 and ECL3. The involved residues include Glu86, Asn89, Phe93, Ala180, His181, Ala185, Phe240, Leu244, Arg255, Leu258, Trp259 and Glu262. Residues such as Glu86, Asn89, Phe93, His181 and Phe240 were also predicted to be key residues in binding of salicin with TAS2R16 by Sakurai et al. [22], proving the reliability of our built structure again.

3.4. Molecular dynamics of complexes

As salicin and probenecid have been verified to be agonist and antagonist for TAS2R16, respectively, they may have different effects on TAS2R16 receptor. Therefore, molecular dynamics
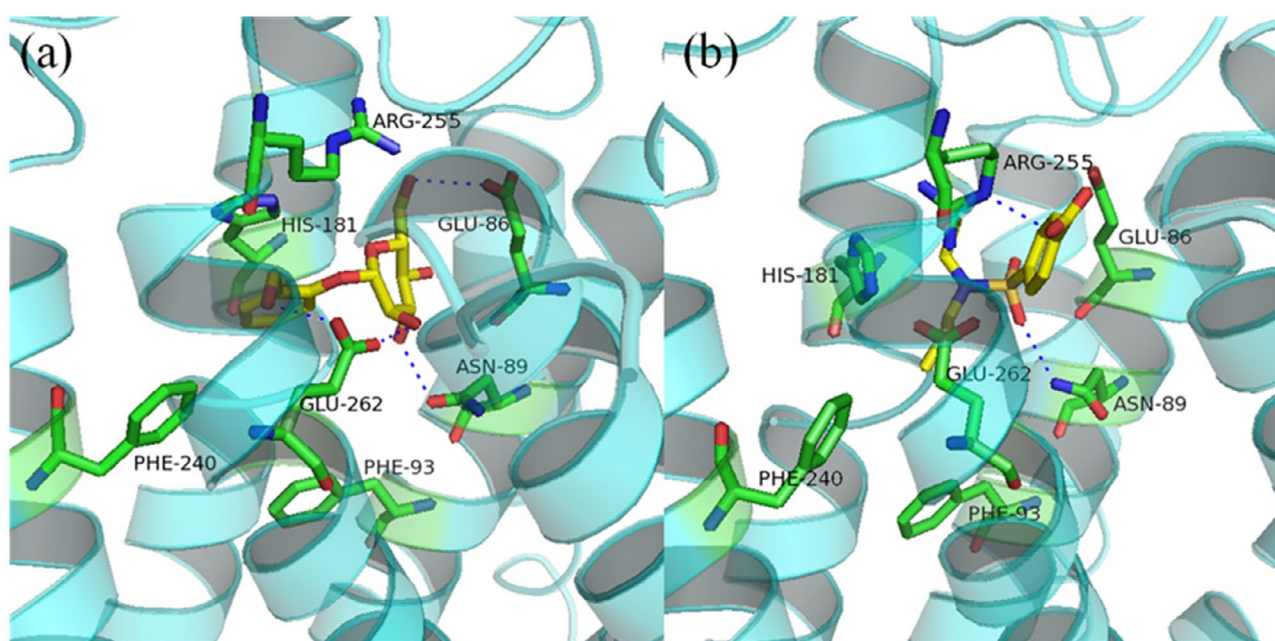
Figure 4. (Colour online) Docking poses of salicin (a) and probenecid (b) to TAS2R16 receptor. The ligands are shown in yellow carbon scheme while residues are shown in green carbon scheme.
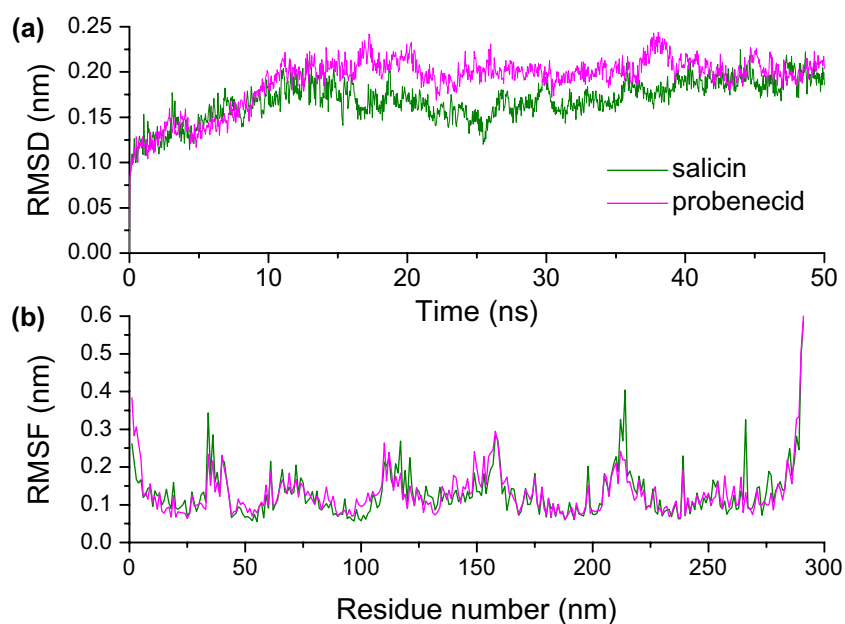

Figure 5. (Colour online) Stability parameters of various TAS2R16 complexes through 50 ns MD simulation. (A) RMSD of backbone atoms and (C) RMSF of each amino acid residues.

simulations were performed on these two ligand-TAS2R16 systems obtained by molecular docking to explore the different roles played by the two ligands.

3.4.1. Stability of two ligand-TAS2R16 systems

Figure 5(a) shows the RMSD value of backbone atoms over simulation time, from which it can be seen that the RMSD of probenecid system increases rapidly to 0.2 nm in 10 ns and then fluctuates around 0.2 nm in the following simulation time. However, the RMSD of salicin increases in the first 10 ns and then decreases to a local minimum at 25 ns or so, and after that it increases again

to 0.20 nm and fluctuates around it. RMSF results display similar sequence for these two systems. Most residues have small RMSF values less than 0.3 nm except the two terminal regions. Salicin has several larger RMSF values than probenecid and the four residues with RMSF larger than 0.3 nm are Arg34, Thr212, His214 and Tyr266. Three of the four residues occur in the intracellular region of TAS2R16: residue Arg34 locates at the first intracellular loop, and Thr212 and His214 locate at the third intracellular loop. Thus, we can see that the larger conformation changes induced by salicin primarily appear in the intracellular region. Tyr266 situates in the central region of TM7, which is near the binding site of TAS2R16.
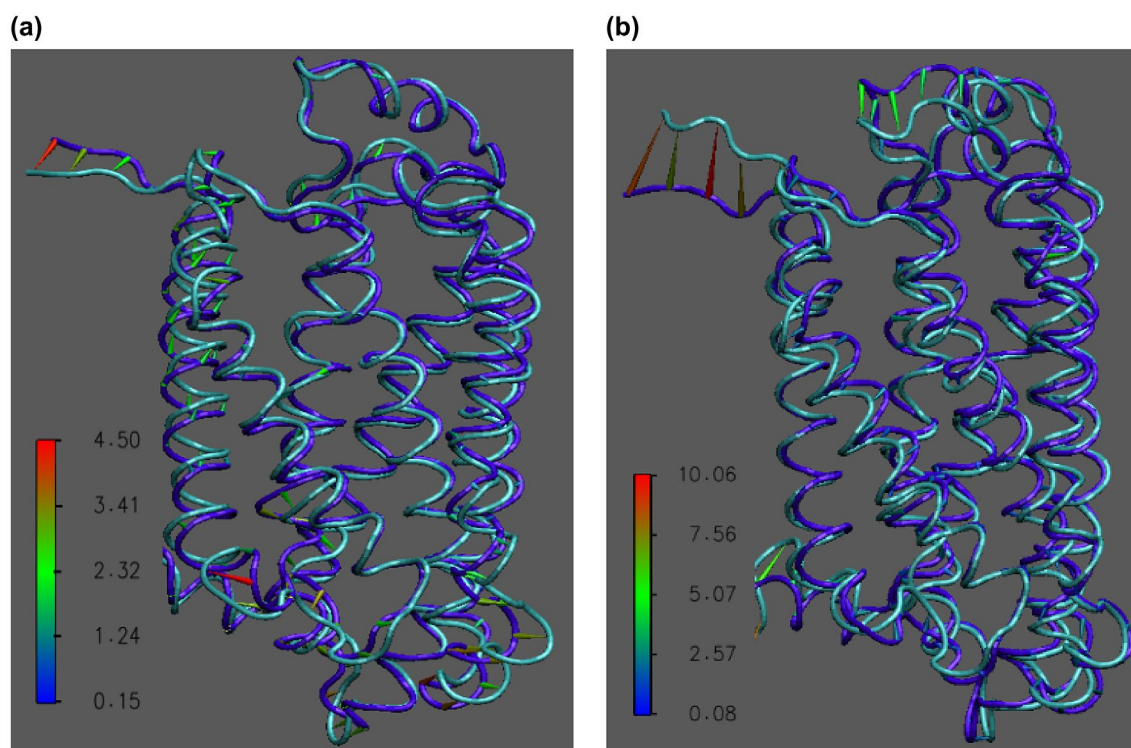
(a)

(b)

Figure 6. (Colour online) Porcupine plots of salicin (a) and probenecid (b). The Cα displacements before and after MD simulation were coloured cyan and violet, respectively.

To analyse the prominent dynamic regions of TAS2R16 with binding of salicin and probenecid during MD simulations, PCA (principal components analysis) of the Cα atoms was performed using gmx covar and gmx anaeig programs. From the top eigenvector, 50 numbers of frames were extracted to generate a porcupine plot. The porcupine plots of salicin-TAS2R16 and probenecid-TAS2R16 from PCA analysis were given in Figure 6. The figure shows that both the N-terminal and the C-terminal of these two systems show large movements, and the movements of probenecid-TAS2R16 are larger as compared to salicin-TAS2R16. Both plots exhibit small movements in seven transmembrane helices, indicating the conformational stability and integrity of TAS2R16 model during the 50 ns MD simulation. This is in agreement with the secondary structure (Figure S3) evolved from the MD trajectory, which displays a good secondary structural conservation for the seven α-helices. Examining these two systems carefully, one can find that the second extracellular loop ECL2 in probenecid-TAS2R16 system has significant variation during MD simulation, whereas it displays little movements in salicin-TAS2R16 system. Another difference between these two systems is that the second and third intracellular loops (ICL2 and ICL3) in salicin-TAS2R16 system show obvious movements, while this is not the case for probenecid-TAS2R16 system. Overall, the major change for salicin-TAS2R16 system takes place in the intracellular region while that for probenecid-TAS2R16 system is in the extracellular region, revealing that binding of TAS2R16 with salicin may induce conformation change of intracellular region of TAS2R16 and thus activate the receptor.

Examining the residues around binding pocket, one can find that Arg255 and Glu262 form a salt bridge. Figure 7 shows the
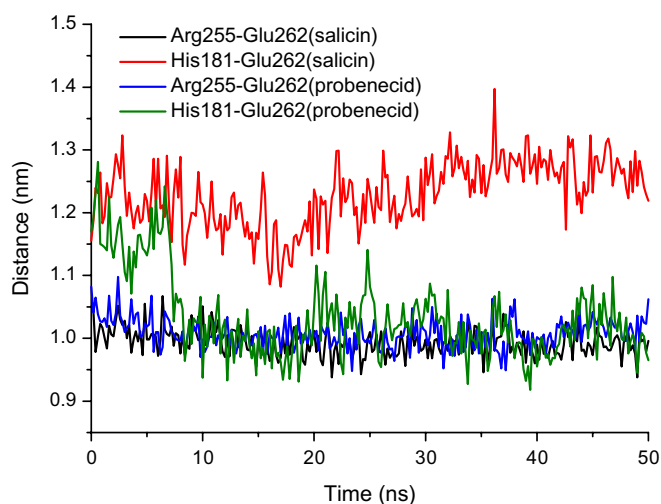

Figure 7. (Colour online) Distance of corresponding Cα atoms between two residues along simulation time.

distance variation between the Cα atoms of two residues vs. simulation time. It can be seen that the salt bridge formed by Arg255 and Glu262 preserves well in both systems. Another salt bridge is created between Glu262 and His181 for probenecid-TAS2R16 system at about 8 ns and maintained till simulation over. However, this salt bridge does not occur for salicin-TAS2R16 system, which may be due to the fact that salicin interacts with Glu262 through hydrogen bond, thus breaking the electrostatic interaction between Glu262 and His181 to some extent. Consequently, the salt bridge Glu262–His181 of probenecid system causes the two corresponding helices TM5 and TM7 approach each other closer as compared to salicin system (Figure S4).
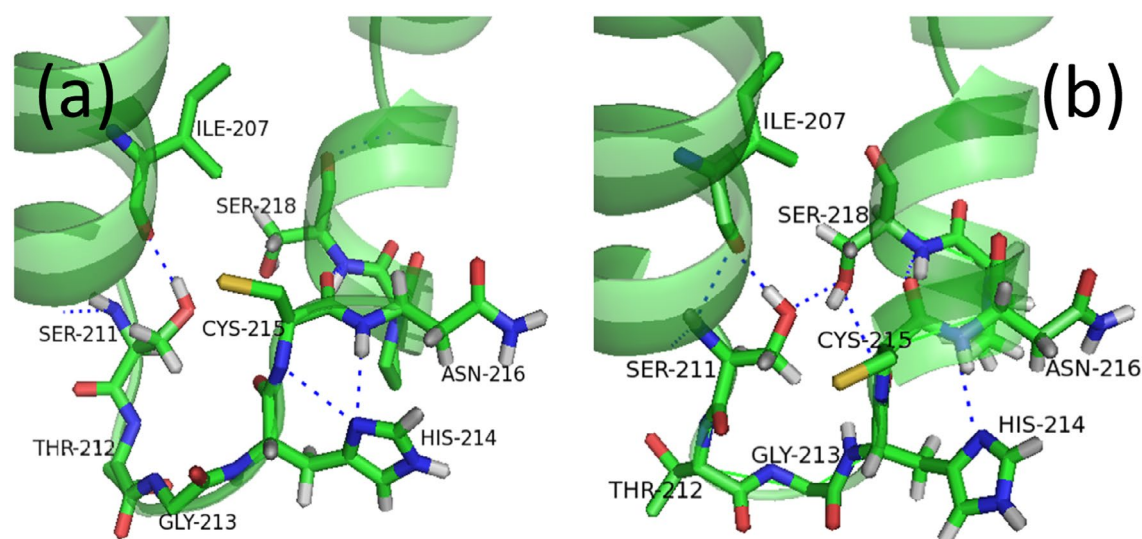
Figure 8. (Colour online) The structure of the third intracellular loop in salicin-TAS2R16 (a) and probenecid-TAS2R16 (b) systems, respectively.

Table 2. The hydrogen bonds occupancy formed between ligands and TAS2R16 receptor.

Complex	Donor	Acceptor	Distance (Å)[a]	Angle (°)[a]	Occupancy[b] (%)
Salicin	O4-H9	OE2(Glu86)	3.339 ± 0.060	152.98 ± 26.44	64.1
	O4-H9	OE1(Glu86)	4.221 ± 0.058	148.77 ± 23.96	21.5
	O7-H18	OE2(Glu262)	2.656 ± 0.007	165.77 ± 7.65	99.6
	O3-H8	O(Glu86)	2.985 ± 0.014	146.12 ± 15.71	72.9
	ND2-HD22(Asn89)	O7	3.085 ± 0.014	140.10 ± 15.38	57.8
	ND2-HD22(Asn89)	O5	3.143 ± 0.018	50.63 ± 8.61	47.0
	ND2-HD22(Asn172)	O6	3.838 ± 0.053	116.69 ± 22.11	21.1
	ND2-HD22(Asn172)	O4	3.830 ± 0.040	121.29 ± 16.82	16.3
	OH-HH(Tyr176)	O3	3.680 ± 0.023	70.28 ± 48.78	13.1
	OH-HH(Tyr266)	O7	3.300 ± 0.24	81.01 ± 58.83	28.3
Probenecid					
	ND2-HD22(Asn89)	O(sulfonyl)	6.136 ± 0.128	63.15 ± 12.83	22.3
	ND2-HD22(Asn89)	O(carboxyl)	4.607 ± 0.152	58.13 ± 17.39	61.8

[a]Average distance of donor–acceptor and average angle of donor-hydrogen-acceptor.
[b]Calculated using readHBmap.py using the last 10 ns trajectories.

As suggested by RMSF results, Thr212 and His214 have larger RMSF value in salicin-TAS2R16 system than in probenecid system. These two residues located at the third intracellular loop ICL3 of TAS2R16, so the conformation change of this loop in different systems simulation was investigated. In the probenecid-TAS2R16 system, Ser211, His214, Asn216 and Ser218 form a network of hydrogen bond interactions (Figure 8(b)). However, in salicin-TAS2R16 system, the sidechain of Ser211 only interacts with the backbone of Ile207, and the hydrogen bond between Ser211 and Ser218 is destroyed, hence leading to the hydrogen bond network broken (Figure 8(a)). Our results show that the network of interactions at the cytoplasmic ends of TM5 and TM6 plays a crucial role in stabilising the inactive state of TAS2R16, which has also been observed in other TAS2Rs. Pydi et al. performed alanine scan mutagenesis of the third intracellular loop of TAS2R4 and found that the cytoplasmic ends of TM5 and TM6 are important in TAS2R activation and mutations in this region such as H214A, leading the receptor to adopt an active conformation [23]. It is well known that loops are the most flexible regions in GPCRs and predicting the loop conformation is very difficult. Therefore, in the absence of other well-characterised agonists and antagonists of TAS2R16, our simulation results offer limited information and should be taken with caution.

3.4.2. Hydrogen bonds between ligands and TAS2R16

As revealed by the docking results, hydrogen bonds play an important role in the binding of salicin and probenecid with TAS2R16 receptor. To investigate the stability of the hydrogen bond during MD simulation, hydrogen bond analysis was carried out. As salicin has four hydroxyl groups on the glucose ring and one hydroxyl group on the phenyl ring, all these five hydroxyl groups participate in hydrogen bond formation with TAS2R16. The hydroxyl group O7-O18 of phenyl ring creates a hydrogen bond with the carboxyl group of Glu262, and the hydrogen bond probability of this hydrogen bond is as high as 99.6%. Glu86 contributes greatly to the binding of TAS2R16 with salicin, involved in three hydrogen bond formation with two hydroxyl groups (O4-H9 and O3-H18) of glucose ring. The other important hydrogen bonds are those formed with the amino group of Asn89. The other less important residues involved in hydrogen bond formation with salicin are Asn172, Tyr176 and Tyr266, with hydrogen bond probability of 16.3, 13.1 and 28.3%, respectively. As indicated previously, Tyr266 displayed large RMSF value for salicin-TAS2R16, which may be correlated with the hydrogen bond formation of salicin and Tyr266.

As for probenecid, there only exist two hydrogen bonds with relative higher presence and both are formed with the amino

group of Asn89: one is with the oxygen atom of sulfonic group and the other is with the oxygen atom of carboxyl group. The occupancy for these two hydrogen bonds is 22.3 and 61.8%, respectively (See Table 2).

3.4.3. Binding free energies

It is well known that the desolvation effect during ligand-protein binding plays a critical role in determining the free energy of the complex. Thus, in this study, the binding free energies of two ligand-receptor complexes were calculated using MM-PBSA method, which has been successfully used in the study of various biomolecular interactions [24–27]. The energy terms contributing to the complex formation can be broadly categorised into polar and non-polar energies. Various energy terms i.e. electrostatic, van der Waals, polar solvation and SASA energies were calculated and listed in Table 3. As shown in Table 3, electrostatic, van der Waals and SASA are negative and polar salvation terms are positive for both complexes, i.e. electrostatic, van der Waals and SASA facilitate the binding while the polar salvation terms oppose the binding. As for salicin-TAS2R16 system, van der Waals interaction is the predominant contributor to the whole binding energy. However, for probenecid-TAS2R16 system, the van der Waals and electrostatic contributions are comparable.

Table 3. MM-PBSA values of calculated systems using the last 10 ns trajectories.

	Energies (kJ/mol)	Salicin	Probenecid
Polar energies	Electrostatic	−84.81 ± 18.73	−149.39 ± 18.44
	Polar solvation	90.82 ± 6.61	26.17 ± 22.70
Non-polar energies	van der Waals	−143.29 ± 11.89	−134.55 ± 10.05
	SASA	−15.52 ± 0.56	−14.12 ± 0.82
Total binding energies		−152.81 ± 15.09	−271.90 ± 26.97

Another difference between these two systems is that the polar solvation energy is much lower for probenecid-TAS2R16 system than for salicin-TAS2R16 system. The binding energies of salicin-TAS2R16 and probenecid-TAS2R16 are −152.81 ± 15.09 and −271.90 ± 26.97 kJ/mol, respectively, suggesting that probenecid binds more tightly with TAS2R16 than salicin.

3.4.4. Energy decomposition

To identify which residues play key roles in binding of different ligands, the energy contribution per residue to the binding energy was calculated (Table S1), which revealed that salicin and probenecid displayed different residue contributions. As for probenecid-TAS2R16 system, the attractive interactions with the basic residues Arg255, Arg162, Arg56, Lys254, Lys169, Arg124, Arg34 and Arg222 stabilised the complex while the repulsive interactions with acidic residues Glu262, Glu17, Glu171, Glu86, Asp168, Asp253, Glu158, Asp46 and Glu35 were against the binding. The absolute values of residue contributions for probenecid-TAS2R16 complex were much larger than those for salicin-TAS2R16 complex, and the stronger stabilisation energy and destabilisation energy counteracted each other. Unlike probenecid-TAS2R16, salicin interacted with residues of various types, and Asn89, Leu185, Ala180, Tyr176 and His181 were the most important residue which contributed −7.67, −6.75, −6.69, 5.25 and 5.14 kJ/mol to the whole binding energy, respectively. These residues also contributed to the probenecid-TAS2R16 complex, but their contributions are much weaker (Figure S5).

Figure 9 shows the energy contribution of TAS2R16 receptor in the binding of salicin and probenecid, from which it can be seen that energy contributions of probenecid-TAS2R16 complex are much stronger than those of salicin-TAS2R16 complex, both for the stabilisation energy and destabilisation energy. Besides,
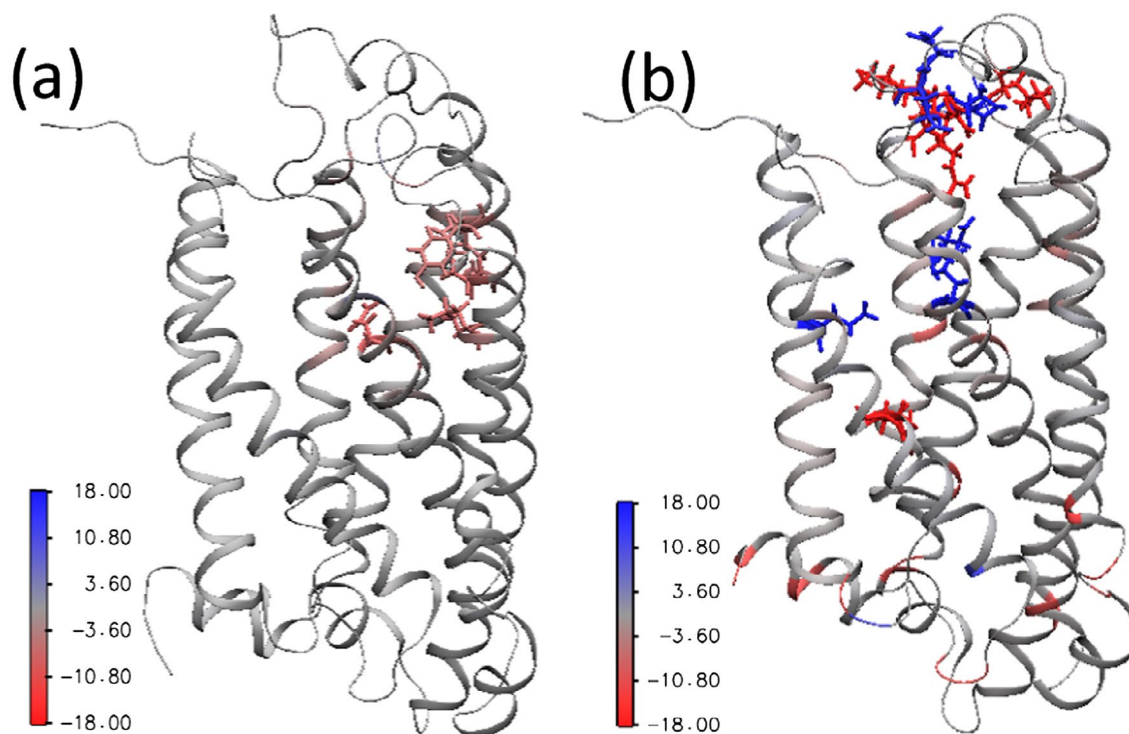

Figure 9. (Colour online) Energy contributions of TAS2R16 receptor in the binding of salicin (a) and probenecid (b). The mapping of energy contribution on the structure is made using *energy2bfac*. Residues with energy in the range of <−5 or >5 kJ/mol for salicin-TAS2R16 and <−15 or >15 kJ/mol for probenecid-TAS2R16 are shown in licorice representation.

the residues strongly interact with salicin are those in the binding site, whereas those interacting with probenecid mainly locate in the extracellular loop region.

4. Conclusion

In this paper, the structure of TAS2R16 receptor was constructed using homology modelling method, and MD simulations were carried out on TAS2R16 in an explicit DPPC bilayer to obtain the equilibrated structure. Salicin and probenecid, which were agonist and antagonist of TAS2R16, were docked to TAS2R16 receptor and MD simulations were performed on these two systems to investigate the structural effect caused by binding of different ligands. The results show that both probenecid and salicin can occupy the TAS2R16 pocket stably during the MD simulation time, and both hydrophobic interactions and hydrogen bond play a role in the interaction between these two ligands and TAS2R16. PCA analysis shows that the major structural change caused by salicin is in the intracellular region while that by probenecid is primarily in the extracellular region. Meantime, the network interactions at the third intracellular loop may play a crucial role in stabilising the inactive state of TAS2R16. Moreover, the binding free energy of probenecid is much lower than salicin. This indicates that a potential antagonist should have obviously stronger binding affinity to TAS2R16, and an agonist should have the ability to induce conformation change of intracellular region of TAS2R16 and thus further activate the receptor. Our calculations may be helpful to better understand the agonist or antagonist mechanism of TAS2R16 receptor, and give insights into the design and discovery of novel antagonist for TAS2R16. Further studies using other well-characterised agonist and antagonist are needed to fully understand the activation mechanism of TAS2R16.

Disclosure statement

No potential conflict of interest was reported by the authors.

References

[1] Dong D, Jones G, Zhang SY. Dynamic evolution of bitter taste receptor genes in vertebrates. BMC Evol Biol. 2009;9:12.

[2] Behrens M, Meyerhof W. Bitter taste receptor research comes of age: From characterization to modulation of TAS2Rs. Semin Cell Dev Biol. 2013;24(3):215–221.

[3] Ji M, Su X, Su X, et al. Identification of novel compounds for human bitter taste receptors. Chem Biol Drug Des. 2014;84(1):63–74.

[4] Adler E, Hoon MA, Mueller KL, et al. A novel family of mammalian taste receptors. Cell. 2000;100:693–702.

[5] Bufe B, Hofmann T, Krautwurst D, et al. The human TAS2R16 receptor mediates bitter taste in response to β-glucopyranosides. Nat Genet. 2002;32(3):397–401.

[6] Dai WM, You ZL, Zhou H, et al. Structure-function relationships of the human bitter taste receptor hTAS2R1: insights from molecular modeling studies. J Recept Signal Transduct Res. 2011;31:229–240.

[7] Pydi SP, Sobotkiewicz T, Billakanti R, et al. Amino acid derivatives as bitter taste receptor (TAS2R) blockers. J Biol Chem. 2014;289(36):2054–2066.

[8] Singla R, Jaitak V. Synthesis of rebaudioside A from stevioside and their interaction model with hTAS2R4 bitter taste receptor. Phytochemistry. 2016;125:106–111.

[9] Born S, Levit A, Niv MY, et al. The human bitter taste receptor TAS2R10 is tailored to accommodate numerous diverse ligands. J Neurosci. 2013;33(1):201–213.

[10] Karaman R, Nowak S, Di Pizio AD, et al. Probing the binding pocket of the broadly tuned human bitter taste receptor TAS2R14 by chemical modification of cognate agonists. Chem Biol Drug Des. 2016;88(1):66–75.

[11] Marchiori A, Capece L, Giorgetti A, et al. Coarse-grained/molecular mechanics of the TAS2R38 bitter taste receptor: experimentally-validated detailed structural prediction of agonist binding. PLoS ONE. 2013;8(5):e64675.

[12] Greene TA, Alarcon S, Thomas A, et al. Probenecid inhibits the human bitter taste receptor TAS2R16 and suppresses bitter perception of salicin. PLoS ONE. 2011;6(5):e20123.

[13] Rasmussen SG, DeVree BT, Zou Y, et al. Crystal structure of the β2 adrenergic receptor–Gs protein complex. Nature. 2011;477:549–555.

[14] Prime, Version 2.1 New York, NY: Schrödinger, LLC; 2009.

[15] Wolf MG, Hoefling M, Aponte-Santamaría C, et al. g_membed: Efficient insertion of a membrane protein into an equilibrated lipid bilayer with minimal perturbation. J Comput Chem. 2010;31:2169–2174.

[16] Lomize MA, Lomize AL, Pogozheva ID, et al. OPM: orientations of proteins in membranes database. Bioinformatics. 2006;22:623–625.

[17] Hess B, Kutzner C, van der Spoel D, et al. GROMACS 4: algorithms for highly efficient, load-balanced, and scalable molecular simulation. J Chem Theory Comput. 2008;4:435–447.

[18] Abraham MJ, Murtola T, Schulz R, et al. GROMACS: high performance molecular simulations through multi-level parallelism from laptops to supercomputers. SoftwareX. 2015;1–2:19–25.

[19] Jämbeck JP, Lyubartsev AP. Derivation and systematic validation of a refined all-atom force field for phosphatidylcholine lipids. J Phys Chem B. 2012;116:3164–3179.

[20] Schrödinger Suite. Induced fit docking protocol; Glide version 5.5 (2009). Prime version 2.1: New York, NY: Schrödinger, LLC; 2009

[21] Kumari R, Kumar R, Consortium OSDD, Lynn A. g_mmpbsa–a gromacs tool for high-throughput MM-PBSA calculations. J Chem Inf Model. 2014;54(7):1951–1962.

[22] Sakurai T, Misaka T, Ishiguro M, et al. Characterization of the β–D-Glucopyranoside binding site of the human bitter taste receptor hTAS2R16. J Bio Chem. 2010;285(36):2873–2878.

[23] Prasad Pydi SP, Singh N, Upadhyaya J, et al. The third intracellular loop plays a critical role in bitter taste receptor activation. Biochim Biopys Acta. 2014;1838:231–236.

[24] Wang QQ, Ning LL, Niu YZ, et al. Molecular mechanism of the inhibition and remodeling of human islet amyloid polypeptide(hIAPP1-37) oligomer by resveratrol from molecular dynamics simulation. J Phys Chem B. 2015;119(1):15–24.

[25] Leonis G, Avramopoulos A, Salmas RE, et al. Elucidation of conformation states, dynamics, and mechanism of binding in human κ-opioid receptor complexes. J Chem Inf Model. 2014;54(8):2294–2308.

[26] Anwar MA, Panneerselvam S, Shah M, et al. Insights into the species-specific TLR4 signaling mechanism in response to Rhodobacter sphaeroides lipid A detection. Sci Rep. 2015;5:7657.

[27] Liu W, Wang HJ, Meng FC. In silico modeling of aspalathin and nothofagin against SGLT2. J Theor Comput Chem. 2015;14(8):1550056.